

# AN ALTERNATIVE METHOD OF INCREASING THE TRANSMISSION PER- FORMANCE OF A CONVENTIONAL 110 kV CABLE LINE

## ALTERNATIVNA METODA ZA POVEĆANJE PRENOSNIH ZMOGLJIVOSTI KONVENCIONALNE 110 kV LINIJE

Dardan Klimenta<sup>1</sup>, Dragan Tasić<sup>2</sup>, Miroљjub Jevtić<sup>1</sup>

**Keywords:** Ampacity, finite-element method (FEM), hydronic asphalt pavement (HAP), power cable, thermal analysis

### **Abstract**

The purpose of this paper is to show that a significant increase in the ampacity of a 110 kV underground cable line is achievable, if a hydronic asphalt pavement system is applied along the entire line, and if the cable trench is completely filled with high thermal conductivity bedding in order to improve the conduction of heat between the line and the surface of the earth. In such a way, it would be possible to simultaneously collect and then store heat from the sun and cable line. The mutual thermal effects between the 110 kV cable line and the hydronic asphalt pavement, in the presence of solar radiation, wind-driven convection and heat emission along the earth surface, are simulated using FEM-based models for the most unfavourable summer conditions and the most common winter conditions. An adequate experimental background is also provided based on the

<sup>3</sup> Corresponding author: Professor, Dardan Klimenta, Tel.: +381 65 40 666 40, Mailing address: Kneza Miloša St. 7, RS-38220 Kosovska Mitrovica, Serbia, E-mail address: [dardan.klimenta@pr.ac.rs](mailto:dardan.klimenta@pr.ac.rs)

<sup>1</sup> University of Priština in Kosovska Mitrovica, Faculty of Technical Sciences, Kneza Miloša St. 7, RS-38220 Kosovska Mitrovica, Serbia

<sup>2</sup> University of Niš, Faculty of Electronic Engineering, Aleksandra Medvedeva St. 14, RS-18000 Niš, Serbia

existing measurements relevant to the thermal analysis performed. It was found that, compared to the associated base cases, the cable ampacity can be increased up to 92.3% for the most unfavourable summer conditions, and up to 60.3% for the most common winter conditions.

## **Povzetek**

Namen prispevka je prikazati možnost doseganja znatnega povečanja zmogljivosti 110 kV podzemnega vodnika, kadar je vzdolž celotne linije uporabljen hidronični asfalt in v kolikor je kabelski jarek popolnoma zapolnjen z visoko toplotno prevodnim ležiščem, ki izboljša prevodnost toplote med vodnikom in zemeljsko površino. Na tak način bi bilo možno hkrati zbirati in shranjevati toploto sonca in vodnika. Medsebojni toplotni učinki med 110 kV vodnikom in hidroničnim asfaltom ob prisotnosti sončnega sevanja, vetrne konvekcije in oddajanja toplote vzdolž zemeljske površine so v prispevku simulirani z uporabo modelov baziranih na MKE. Za vremenske pogoje so izbrane najbolj neugodne poletne razmere in najpogostejše zimske razmere. Zagotovljeno je ustrezno eksperimentalno ozadje na podlagi obstoječih meritev, ki se nanašajo na opravljeno toplotno analizo. Ugotovljeno je bilo, da je možno na tak način v primerjavi s trenutno izvedbo zmogljivost vodnikov za najbolj neugodne poletne razmere povečati do 92,3 %, za najpogostejše zimske razmere pa do 60,3 %.

## **1 INTRODUCTION**

A hydronic asphalt pavement (HAP) system represents an emerging renewable energy technology, i.e., an innovative method for harvesting energy of the sun, [1]. It consists of four main parts, [2]: (i) a heat exchanger, i.e. a pavement-solar heat collecting system, (ii) a heat storage system, (iii) a hydronic circulating pump, and (iv) an automatic monitoring system. Fig. 1 provides a detailed depiction of the operating principle of the HAP system, which includes the cooling of pavement in summer, storing the heat in the ground, and the heating of pavement in winter. Since the earth's surface above power cables usually does not freeze during winter, pavement heating using the HAP system is not relevant for that period. Therefore, it is assumed that all collected heat is used for various applications in buildings and process plants or for thermoelectric conversion.

Together with solar energy, the HAP system from Fig. 1 may simultaneously collect some waste heat from power cables if they are installed below the heat exchanger. Collecting both can decrease the surface temperature of the pavement above power cables by approximately 10 °C when compared with the surface temperature of conventional pavement, [1]. This experimental observation refers to dynamic thermal analysis. This means that the difference corresponding to the steady-state thermal analysis is significantly higher, which makes it possible to use the HAP system in order to increase the cable ampacity under different environmental conditions.

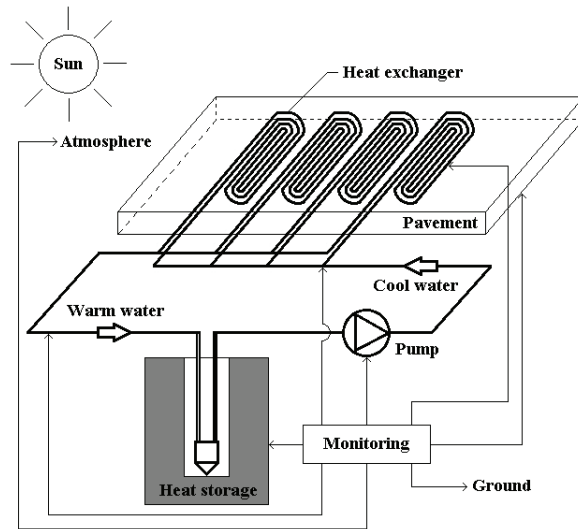


**Figure 1:** Operating principle of the HAP system [1,2]

This paper considers the possibility of increasing the ampacity of the 110 kV underground cable line by an application of the HAP system, under the most unfavourable summer conditions and the most common winter conditions. It is assumed that the HAP system is applied along the entire cable line and that the cable trench is completely filled with one of four different bedding materials with high thermal conductivities. FEM-based models in which the cable beddings have a standard size of  $1.2 \text{ m} \times 0.65 \text{ m}$  are used as the base cases for the summer and winter periods. Finally, the steady-state thermal analysis reached a number of interesting conclusions.

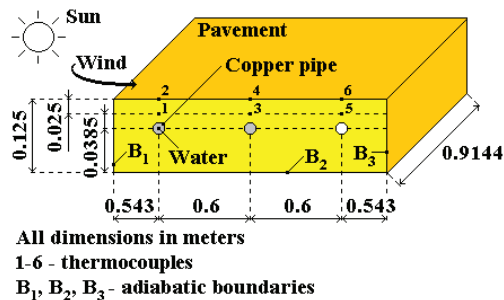
## 2 FEM-BASED STEADY-STATE THERMAL MODELS

Fig. 2 illustrates a cross-sectional view of the experimental apparatus that was used in [1] for testing HAP system performance. The experiment is relevant for the validation of the model proposed herein. According to [1], the experiment was conducted with the following environmental conditions and material properties:

- (i) temperature of the air contacting the pavement surface  $T_a=32.93 \text{ }^\circ\text{C}$ ;
- (ii) heat transfer coefficient due to wind-driven convection  $h=6 \text{ W}/(\text{m}^2\cdot\text{K})$ ;
- (iii) solar irradiance incident on the pavement surface  $Q_{s,s}=800 \text{ W}/\text{m}^2$ ;
- (iv) solar absorptivity and thermal emissivity of the pavement surface  $\alpha=0.90625$  and  $\varepsilon=0.9$ , respectively;
- (v) water temperature at inlets of the heat collecting pipes  $T_{w,i}=23.2 \text{ }^\circ\text{C}$ ;
- (vi) water temperature at outlets of the heat collecting pipes  $T_{w,o}=28.2 \text{ }^\circ\text{C}$ ;
- (vii) water velocity in the heat collecting pipes  $v_w=0.06 \text{ m/s}$  or  $v_w=1 \text{ l/min}$ ;

- (viii) thermal conductivity of the water flowing through the pipe indicated by a white circle in Fig. 2  $k=0.61331 \text{ W}/(\text{m}\cdot\text{K})$  – at  $T_w=(T_{w,i}+T_{w,o})/2=25.7 \text{ }^\circ\text{C}$ ;
- (ix) thermal conductivity of the still water in the pipes indicated by grey circles in Fig. 2  $k=0.64399 \text{ W}/(\text{m}\cdot\text{K})$  – at  $50 \text{ }^\circ\text{C}$ ;
- (x) thermal conductivity of the copper pipe  $k=385 \text{ W}/(\text{m}\cdot\text{K})$ , and
- (xi) thermal conductivity of the limestone asphalt mixture/pavement  $k=1.583 \text{ W}/(\text{m}\cdot\text{K})$ .

The inner and outer diameters of the copper pipes (i.e., heat collecting pipes) are equal to  $d_{p,i}=0.019 \text{ m}$  and  $d_{p,o}=0.0222 \text{ m}$ , respectively.



**Figure 2:** A cross-sectional view of the experimental apparatus used in [1] for testing HAP system performance (not to scale). Note: In this experiment, water was not flowing through the two pipes indicated by grey circles, while water was flowing through the pipe indicated by a white circle

Fig. 3a shows the computational domain used for the two base cases, while Fig. 3b shows the computational domain used for the proposed alternative method with a HAP system consisting of seven copper pipes. The first base case relates to the following environmental conditions and material properties, [3,4]: (i)  $T_a=40 \text{ }^\circ\text{C}$ ; (ii) wind velocity  $v_a=0.22 \text{ m/s}$ ; (iii)  $Q_{s,s}=1000 \text{ W/m}^2$ ; (iv) temperature of referent soil of  $T_{rs}=20 \text{ }^\circ\text{C}$ ; and (v) thermal conductivities of the cable bedding, backfill, native soil and conventional asphalt pavement amounting, respectively, to  $1 \text{ W}/(\text{m}\cdot\text{K})$ ,  $0.4 \text{ W}/(\text{m}\cdot\text{K})$ ,  $0.4 \text{ W}/(\text{m}\cdot\text{K})$  and  $1.2 \text{ W}/(\text{m}\cdot\text{K})$ . These conditions represent the most unfavourable summer conditions. The second base case relates to the most common winter conditions, namely [4]:  $T_a=5 \text{ }^\circ\text{C}$ ,  $v_a=0.22 \text{ m/s}$ ,  $Q_{s,s}=500 \text{ W/m}^2$ ,  $T_{rs}=10 \text{ }^\circ\text{C}$ , and thermal conductivities of the cable bedding, backfill, native soil and conventional asphalt pavement amounting, respectively, to  $1 \text{ W}/(\text{m}\cdot\text{K})$ ,  $0.4 \text{ W}/(\text{m}\cdot\text{K})$ ,  $0.4 \text{ W}/(\text{m}\cdot\text{K})$  and  $1.2 \text{ W}/(\text{m}\cdot\text{K})$ .

The cables in Fig. 3 are of the type AXLJ  $1\times 1000/190 \text{ mm}^2$  64/110 kV. All the construction elements of these cables are described in [3]. For the purposes of simulations using the COMSOL software, these cables are modelled with an equivalent construction composed of the aluminium conductor, cross-linked polyethylene (XLPE) insulation, copper screen, and outer polyethylene (PE) sheath with outer radii 19.2 mm, 35.65 mm, 38.35 mm and 42.15 mm, respectively, as well as with thermal conductivities  $239 \text{ W}/(\text{m}\cdot\text{K})$ ,  $0.286 \text{ W}/(\text{m}\cdot\text{K})$ ,  $385 \text{ W}/(\text{m}\cdot\text{K})$  and  $0.286 \text{ W}/(\text{m}\cdot\text{K})$ . In addition, it is assumed that dimensions and thermal conductivities of the blocks representing the HAP system in Fig. 3b correspond to the ones from Fig. 2.

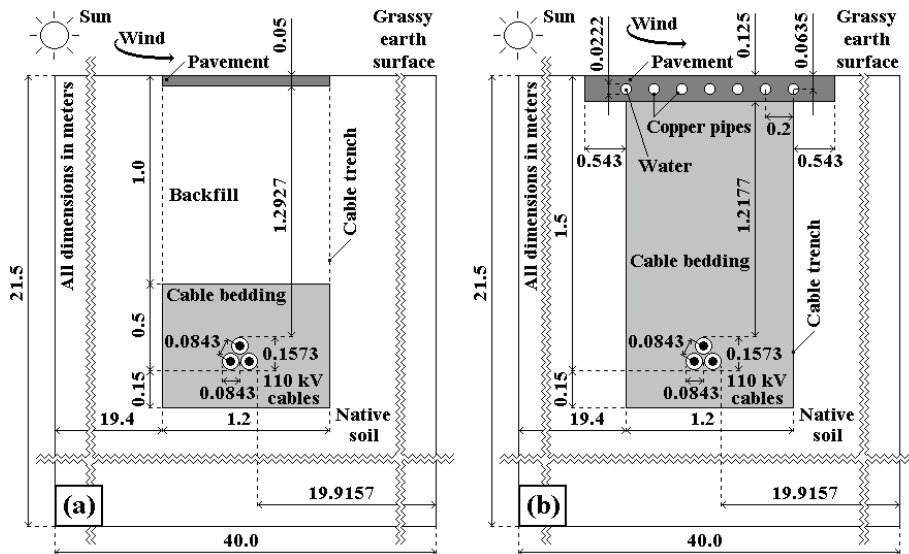


**Figure 3:** Presentation of the computational domains for (a) base cases, and (b) proposed method with a HAP system consisting of the same seven copper pipes (not to scale)

The governing equation for 2D FEM-based modelling of steady-state heat transfer has the following form [3,4]:

$$\frac{\partial}{\partial x} \left( k \frac{\partial T}{\partial x} \right) + \frac{\partial}{\partial y} \left( k \frac{\partial T}{\partial y} \right) + Q_v = 0 \quad (2.1)$$

where  $T$  is the unknown temperature in K;  $x, y$  are the Cartesian spatial coordinates in m; and  $Q_v$  is the volume power of heat sources in  $W/m^3$ . The thermal conductivities of all bedding materials appearing in the FEM-based models are listed in Table 1. The governing equation is non-linear due to the existence of the radiation boundary conditions.

All the required material and surface properties are constant and selected so that the obtained results are optimistic from the engineering point of view. Accordingly, the values of the thermal and electrical conductivities which correspond respectively to the associated dried-out states (of the cable bedding and the native soil) and the continuously permissible temperature ( $T_{cp}=90$  °C) are taken into account.

**Table 1:** Thermal conductivity of all used bedding materials in the dried-out state

Cable bedding material	$k$
	W/(m·K)
Fine aggregate, Serbian standard [5]	1
Fine aggregate, US standard [6]	1.47
Limestone fine aggregate [7]	2.15
Quartzite fine aggregate [7]	5.38

The volume power of heat sources  $Q_v$  in each 110 kV conductor with a radius of 19.2 mm and a geometric cross-section area of  $S_c=1158.117 \cdot 10^{-6} \text{ m}^2$  is

$$Q_v = \frac{R_{ac}(T_{cp})}{S_c} \cdot I^2 \quad (2.2)$$

where  $R_{ac}(T_{cp})=40.91094 \cdot 10^{-6} \text{ } \Omega/\text{m}$  is the effective conductor resistance to the flow of alternating current per unit length of each 110 kV cable at  $T_{cp}=90 \text{ } ^\circ\text{C}$ , and  $I$  is the ampacity or load current in A. The a.c. resistance takes into account the skin and proximity effects, as well as losses in the metal screen. According to the facts given in [3,4], the volume powers of heat sources in the cable insulation and metal screens of the 110 kV cables are equal to zero.

The adiabatic boundary condition:

$$k \cdot \frac{\partial T}{\partial n} = 0 \quad (2.3)$$

is used to model boundaries surrounding the left-hand, bottom and right-hand sides of the two domains in Fig. 3, where the constant temperature boundary condition:

$$T = T_0(x, y) = T_{rs} + 273.15 \quad (2.4)$$

also needs to be satisfied simultaneously [3,4]. In the Eqn. (2.3) and Eqn. (2.4),  $n$  is the length of the normal vector  $\vec{n}$  in m, while  $T$  and  $T_0$  are the unknown and specified temperatures of the corresponding boundaries in K, respectively.

The heat transfer along the earth and pavement surfaces is represented by a combination of the convection boundary condition:

$$k \cdot \frac{\partial T}{\partial n} = h \cdot (T - T_a) \quad (2.5)$$

and the radiation boundary condition:

$$k \cdot \frac{\partial T}{\partial n} = \varepsilon \cdot \sigma_{SB} \cdot T^4 - \alpha \cdot Q_{S,s} \quad (2.6)$$

where  $T$  is the unknown surface temperature of the earth or pavement in K,  $\alpha=0.6$  and  $\varepsilon=0.94$  are the solar absorptivity and thermal emissivity for a dry grassy surface,  $\alpha=0.87$  and  $\varepsilon=0.93$  are the solar absorptivity and thermal emissivity for the asphalt surfaces in Fig. 3,  $h=12.654 \text{ W}/(\text{m}^2 \cdot \text{K})$  is the heat transfer coefficient due to convection for a dry grassy surface when  $v_a=0.22 \text{ m/s}$ ,  $h=8 \text{ W}/(\text{m}^2 \cdot \text{K})$  is the heat transfer coefficient due to convection for the asphalt surfaces in Fig. 3 when  $v_a=0.22 \text{ m/s}$ , and  $\sigma_{SB}=5.67 \cdot 10^{-8} \text{ W}/(\text{m}^2 \cdot \text{K}^4)$  is the Stefan-Boltzmann constant. More details relating to the boundary conditions (3-6) can be found in [3,4].

The heat transfer between the inner surfaces of the heat collecting pipes and the water flowing through them is represented by the following convection boundary condition:

$$k \cdot \frac{\partial T}{\partial n} = h \cdot (T - T_w) \quad (2.7)$$

where  $T$  is the unknown temperature of the corresponding inner boundary in K, which is also higher than  $T_w=(T_{w,i}+T_{w,o})/2$ . Accordingly, the associated Reynolds number  $Re$  and heat transfer coefficient  $h$  are

$$\text{Re} = \frac{v_w \cdot d_{p,i}}{\nu} < \text{Re}_{cr} = 2300 \quad (2.8)$$

$$h = \frac{3.66 \cdot k}{d_{p,i}} \quad (2.9)$$

where  $k$  is the thermal conductivity of water at  $T_w$  in W/(m·K),  $\nu$  is the kinematic viscosity of water at  $T_w$  in m<sup>2</sup>/s, and  $\text{Re}_{cr}$  is the critical Reynolds number for smooth pipes. Therefore, the wall temperature of each copper pipe is assumed to be constant. The values of  $k$ ,  $\nu$ ,  $\text{Re}$  and  $h$  respectively amount to 0.61331 W/(m·K),  $8.5776 \cdot 10^{-7}$  m<sup>2</sup>/s, 1329.04 and 118.14 W/(m<sup>2</sup>·K) for  $T_w=25.7$  °C.

### 3 RESULTS AND OBSERVATIONS

The results obtained by simulating the temperature distribution over the transverse cross-section of the experimental apparatus (Fig. 2) for the known environmental and operating conditions are shown in Figs. 4a and 4b. It is found that the temperature of the surface above the pipes can be decreased by about 12.9 °C with the flowing of water. In comparison with the corresponding experimental result of the dynamic thermal analysis, [1], this temperature is higher by about 2.9 °C and represents the maximum possible value that can be reached for  $T_{w,i}=23.2$  °C. According to [8], for  $T_{w,i}=13$  °C, the temperature of the surface above the pipes can be decreased by about 18 °C.

However, there are parts of the asphalt pavement surface between the pipes whose temperature is decreased by only 3.7 °C. One way of overcoming this is to increase the number of pipes filled with flowing water. Fig. 4c shows temperature distribution over a domain having seven copper pipes filled with flowing water. The domain and pipes have the same dimensions as those in Fig. 2. In this case, the temperature of the entire surface above the seven copper pipes can be decreased by 14-16 °C. This observation is significant, because it indicates that it is possible to reduce the amount of heat radiated back from the pavement surface.

How the HAP system affects the conductor temperature and load current of the 110 kV cables can best be illustrated by concrete examples of the temperature field distribution over the two computational domains in Fig. 3. Accordingly, Figs. 5a and 5b show the temperature field distributions over the domains in Figs. 3a and 3b, respectively. The temperature distribution in Fig. 5a is obtained for the environmental conditions and material properties corresponding to the first base case (i.e., for the most unfavourable summer conditions). In addition, the result in Fig. 5b is obtained for the same environmental conditions and thermal conductivities of the cable bedding, native soil and limestone asphalt mixture/pavement amounting, respectively, to 5.38 W/(m·K), 0.4 W/(m·K) and 1.583 W/(m·K). In both simulations, the volume powers of heat sources and load currents were  $Q_v=10250$  W/m<sup>3</sup> and  $I=538.7$  A, respectively.

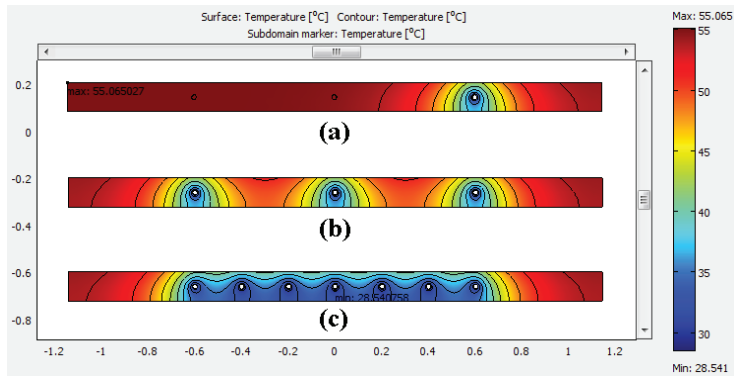


**Figure 4:** Temperature distribution over the domain in Fig. 2 for cases when (a) water flows through only one of the three pipes, and (b) water flows through each of the three pipes; (c) temperature distribution over a domain having seven copper pipes filled with flowing water

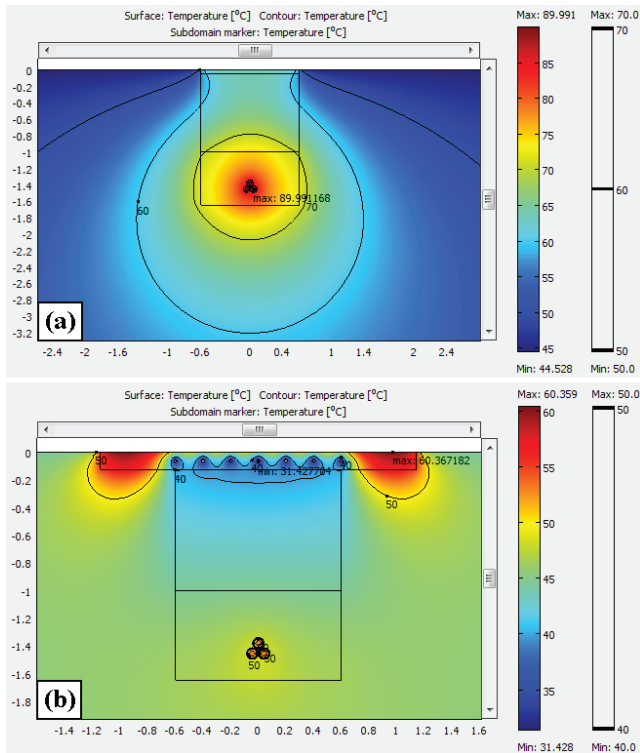


**Figure 5:** Temperature distributions over the domains shown in (a) Fig. 3a, and (b) Fig. 3b

According to Fig. 5, the HAP system in combination with the cable trench that is completely filled with fine quartzite aggregate affects the load current of the 110 kV cable line to a considerable extent. In particular, with the installation of the HAP system, the maximum



system above the 110 kV cable line can be used simultaneously to control the ampacity and to collect heat from the sun and cables.

For the purpose of determining the ampacity of the 110 kV cable line  $I_{cp}$ , a sequence of simulations over the two computational domains (in Figs. 3a and 3b) is performed with the thermal conductivities of the selected cable bedding materials (Table 1), for the most unfavourable summer conditions and the most common winter conditions. The values for  $Q_v$  are gradually increased from an arbitrary prescribed initial value (e.g., 10 kW/m<sup>3</sup>) to its continuously permissible value (corresponding to the temperature  $T_{cp}=90$  °C). The volume powers of heat sources  $Q_v$  obtained in this manner are listed in Table 2. Then, these volume powers of heat sources and the Eqn. (2.2) are used to calculate the corresponding cable ampacities (for  $I=I_{cp}$ ). The ampacities  $I_{cp}$  of the considered 110 kV cable line are also listed in Table 2. In order to simplify comparisons between the results, the inlet water temperature is assumed to be constant (at 23.2 °C), regardless of the environmental conditions considered.

**Table 2:** Volume powers of heat sources in cable conductors and corresponding ampacities estimated for the computational domains in Figs. 3a and 3b, different cable bedding materials and different environmental conditions

Cable bedding material	Computational domain	Results obtained for the most unfavourable summer conditions		Results obtained for the most common winter conditions	
		$Q_v$	$I=I_{cp}$	$Q_v$	$I=I_{cp}$
$k$		W/m <sup>3</sup>	A	W/m <sup>3</sup>	A
1	Fig. 3a	10250	538.7	21185	774.4
1	Fig. 3b	14680	644.6	23735	819.7
1.47	Fig. 3b	18520	724.1	28985	905.8
2.15	Fig. 3b	23195	810.3	35225	998.6
5.38	Fig. 3b	37910	1035.9	54465	1241.7

## 4 CONCLUSION

The most important conclusions that can be drawn from the presented results are:

- If the conventional asphalt pavement above the 110 kV cable line is changed with the HAP system, combined with the cable trench that is completely filled with the high thermal conductivity bedding, then the corresponding ampacity can be increased up to 497.2 A for the most unfavourable summer conditions and up to 467.3 A for the most common winter conditions.
- HAP systems can be used to control the thermal environment of underground cable lines in order to increase their ampacities.
- The proposed innovative method is new, it can be easily implemented within current practices, and it would result in significant financial and engineering benefits.

## Acknowledgements

This paper was based on research conducted within the project TR33046 funded by the Ministry of Education, Science, and Technological Development of the Republic of Serbia.

## References

- [1] **R.B. Mallick, B.-L. Chen, S. Bhowmick:** *Harvesting heat energy from asphalt pavements: development of and comparison between numerical models and experiment*, International Journal of Sustainable Engineering, Vol. 5, Issue 2, pp. 159-169, 2012
- [2] **Z. Zhou, X. Wang, X. Zhang, G. Chen, J. Zuo, S. Pullen:** *Effectiveness of pavement-solar energy system – An experimental study*, Applied Energy, Vol. 138, pp. 1-10, 2015
- [3] **D. Klimenta, B. Perović, J. Klimenta, M. Jevtić, M. Milovanović, I. Krstić:** *Controlling the thermal environment of underground cable lines using the pavement surface radiation properties*, IET Generation, Transmission and Distribution, Vol. 12, Issue 12, pp. 2968–2976, 2018
- [4] **D.O. Klimenta, B.D. Perović, J.Lj. Klimenta, M.M. Jevtić, M.J. Milovanović, I.D. Krstić:** *Controlling the thermal environment of underground power cables adjacent to heating pipeline using the pavement surface radiation properties*, Thermal Science, Vol. 22, Issue 6, pp. 2625–2640, 2018
- [5] **D. Klimenta, S. Nikolajević, M. Sredojević:** *Controlling the thermal environment in hot spots of buried power cables*, European Transactions on Electrical Power, Vol. 17, Issue 5, pp. 427–449, 2007
- [6] **S.Y. King, N.A. Halfter:** *Underground Power Cables*, 1<sup>st</sup> edition, Longman, London and New York, 1982
- [7] **R.B. Mallick, B.-L. Chen, S. Bhowmick, M.S. Hulén:** *Capturing solar energy from asphalt pavements*, The International ISAP Symposium on Asphalt Pavements and Environment (ISAP 2008), Zurich, Switzerland, August 18-20, 2008
- [8] **D. Klimenta, D. Tasić, M. Jevtić:** *Increasing the ampacity of a 110 kV underground cable line by an application of a hydronic asphalt pavement system*, The 14<sup>th</sup> International Conference on Applied Electromagnetics - ПЕC 2019, Niš, Serbia, August 26-28, 2019

## Nomenclature

Symbol	Symbol meaning
$d_{p,i}$	inner diameter of the heat collecting pipe, in m
$d_{p,o}$	outer diameter of the heat collecting pipe, in m
$h$	heat transfer coefficient due to convection, in W/(m <sup>2</sup> ·K)
$I$	load current, in A
$I_{cp}$	ampacity, in A

$n$	length of the normal vector $\vec{n}$ , in m
$\vec{n}$	normal vector
$Q_{S,s}$	solar irradiance, in $W/m^2$
$Q_v$	volume power of heat sources, in $W/m^3$
$R_{ac}$	effective conductor resistance to the flow of alternating current per unit length of each 110 kV cable at $T_{cp}=90$ °C, in $\Omega/m$
$Re$	Reynolds number, dimensionless
$Re_{cr}$	critical Reynolds number, dimensionless
$S_c$	geometric cross-section area of each 110 kV conductor, in $m^2$
$T$	unknown temperature, in K
$T_0$	specified temperature, in K
$T_a$	temperature of the air contacting the pavement surface, in K or °C
$T_{cp}$	continuously permissible temperature, in °C
$T_{rs}$	temperature of referent soil, in °C
$T_w$	average temperature of water flowing inside the heat collecting pipe, in K or °C
$T_{w,i}$	inlet water temperature, in K or °C
$T_{w,o}$	outlet water temperature, in K or °C
$v_a$	wind velocity, in m/s
$v_w$	water velocity, in m/s or l/min
$x, y$	Cartesian spatial coordinates, in m
$\alpha$	solar absorptivity, dimensionless
$\varepsilon$	thermal emissivity, dimensionless
$\nu$	kinematic viscosity of water, in $m^2/s$
$\sigma_B$	Stefan-Boltzmann constant, in $W/(m^2 \cdot K^4)$